Journal of Peptide Science, Vol. 4, 58–71 (1998)

Conformational Investigations on Glycosylated Threonine-oligopeptides of Increasing Chain Length

LAURA BIONDI, FERNANDO FILIRA, MARINA GOBBO, ENRICO PAVIN and RANIERO ROCCHI

Biopolymer Research Centre, CNR, Department of Organic Chemistry, University of Padova, Padova, Italy

Received 2 April 1997
Accepted 26 May 1997

Abstract: Stepwise solution syntheses are described of the homo-oligomers Z-(Thr)$_n$-NHCH$_3$ (n=1–4, $\mathbf{I}_{1-4}$), Z-{[Gal(Ac)$_4\beta$]Thr}$_n$-NHCH$_3$(n=1–5, $\mathbf{II}_{1-5}$) and Z-[(Galβ)Thr]n-NHCH$_3$ (n=1–5, $\mathbf{III}_{1-5}$). Members of the $\mathbf{III}_{1-5}$ series were obtained by de-acetylation of the corresponding oligomers of the $\mathbf{II}_{1-5}$ series. The conformational preferences of the terminally protected homo-peptides of the three series were investigated by FT-IR absorption spectroscopy both in the solid state and in $CDCl_3$ solution, at various concentrations. Proton NMR measurements in $CDCl_3$ and in DMSO-d_6 were also carried out and the effect of temperature variation on the chemical shifts of amide protons was determined in DMSO-d_6 (range 298–335 K) and in $CDCl_3$ (range 298–320 K). CD spectra were recorded in water and in TFE. Solubility problems prevented measurements in $CDCl_3$ solution for Z-(Thr)$_4$-NHCH$_3$ and for the entire $\mathbf{III}_{1-5}$ series. The existence of unordered structures in the carbohydrate-free oligomers and of more or less extended, organized structures in the glycosylated derivatives is indicated by the NMR and IR measurements. The sugar moieties apparently show a structure-inducing effect on the peptide chain. ©1998 European Peptide Society and John Wiley & Sons, Ltd.

J. Pep. Sci. 8: 58–71 (1998)

Keywords: circular dichroism; FT-IR absorption; glycopeptides; ^{1}H nuclear magnetic resonance; oligopeptides; peptide conformation

INTRODUCTION

The ubiquitous occurrence of glycoproteins reflects their vital role in a variety of physiological and pathological processes. The carbohydrate moieties are involved in some biological functions displayed by glycoproteins but little information is available about their role on the conformational features of these glycoconjugates. The detailed knowledge of the three-dimensional structure of glycoproteins is essential not only to understand important physiological functions such as enzymatic catalysis, hormone control, ion transport, cell adhesion, intercellular interaction and cell recognition, but also for a rational design of pharmacologically active glycopeptides.

We have already described [1] the synthesis and a series of ring-opening polymerization of the sugar-

Abbreviations: AcOEt, ethyl acetate; CD, circular dichroism; DCM, dichloromethane; DMAP, 4-dimethylaminopyridine; EDC, *N*-(3-dimethylaminopropyl), N^1-ethyl-carbodiimide; Et_3N, triethylamine; Gal, D-galactopyranosyl; Gal(Ac)$_4$, 2,3,4,6-tetra-*O*-acetyl-D-galactopyranosyl; GlcNAc(Ac)$_3$,2-acetamido-3,4,6-tri-*O*-acetyl-2-deoxy-D-glucopyranosyl; NCA, *N*-carboxyanhydride; Su, 1-succinimidyl; TDM, 4,4^1-tetramethyldiaminodiphenylmethane; TEMPO, 2,2,6,6-tetramethyl-piperidine-1-oxyl; TFE, 2,2,2-trifluoroethanol; TLC, thin layer chromatography. Standard abbreviations for amino acid derivatives, peptides and glycopeptides are according to the rules of the IUPAC-IUB Commission on Biochemical Nomenclature: (1984) *Eur. J. Biochem. 138,* 9–37, and (1985) *J. Biol. Chem. 262,* 13–18.

Address for correspondence: Prof. Raniero Rocchi, Department of Organic Chemistry, University of Padova, via Marzolo, 1–35131 Padova, Italy.

CCC 1075-2617/98/010058–14

substituted α-amino acid NCA, [GlcNAc(Ac)$_3$β]Asn-NCA and [Gal(Ac)$_4$β]Thr-NCA. The resulting polymers were fractionated by dialysis and preliminary conformational studies were carried out on samples of different molecular weight. CD spectra, in water, and in TFE, reflect the existence of a random coil-ordered structure equilibrium, largely shifted towards the unordered structure. Observations based on FT-IR spectra in $CDCl_3$ offered support to the existence of intramolecularly H-bonded folded species. For a better understanding of the conformational properties of the glycosylated polymers, the following homo-oligomers were prepared: Z-(Thr)$_n$–$NHCH_3$ (n=1–4; **I**$_{1–4}$), Z-{[Gal(Ac)$_4$β]Thr$_n$–$NHCH_3$ (n=1–5; **II**$_{1–5}$) and Z-[(Galβ)Thr]n-$NHCH_3$ (n=1–5; **III**$_{1–5}$). Members of the **III**$_{1–5}$ series were obtained by deacetylation of the corresponding oligomers of the **II**$_{1–5}$ series. The limited length of the homo-oligopeptides and the need to isolate and characterize each oligomer during chain elongation suggested the exploitation of the classical stepwise synthesis in solution for preparing both the glycosylated and the non-glycosylated series. The use of the *N*-methylamide derivative of the C-terminal residue allowed us to introduce an extra amide bond, besides peptide linkages, in the sequences. Alternate removal of the benzyloxycarbonyl N-protecting group by catalytic hydrogenation of the growing peptide chain and coupling of a new residue by the EDC-HOBt procedure allowed us to prepare peptides containing the desired number of either side-chain unprotected or *O*-glycosylated Thr residues. The conformational preferences of the terminally protected homo-peptides of the three series were investigated by FT-IR spectroscopy, both in the solid state and in a solvent of low polarity such as $CDCl_3$, at various concentrations. Proton NMR measurements in $CDCl_3$ and DMSO-d$_6$ were also carried out and CD spectra were recorded in water and in TFE. Owing to the insolubility of Z-(Thr)$_4$-$NHCH_3$ and of the entire **III**$_{1–5}$ series in $CDCl_3$, solution measurements in this solvent were only possible for the **I**$_{1–3}$ and **II**$_{1–5}$ series.

MATERIALS AND METHODS

Z-Thr-OH was obtained from Novabiochem and acetic anhydride, DMAP, EDC, HOBt, hydrazine hydrate and 1,2-pentandione were Fluka products, Z-OSu and 1,2,3,4,6-penta-*O*-acetyl-β-D-galactopyranose were purchased from Senn Chemical, and *O*-methyl-β-D-galactopyranoside from Sigma. HOBt-NH_2CH_3 was prepared by the procedure already described [2] for the preparation of the corresponding salt of *N*-hydroxysuccinimide. All other chemicals were of the best grade commercially available. Melting points were taken on a Buchi mod. 150 apparatus in open capillary and are not corrected. Optical rotations were determined with a Perkin Elmer mod. 241 polarimeter. Ascending thin layer chromatographies were performed on Merck F254 silica plates using the following solvent systems:

E1: chloroform/methanol/acetic acid (9:0.8:0.2 by vol.)

E2: ethyl acetate/butan-1-ol/acetic acid/water (5:3:1:1 by vol.)

E3: methylene chloride/acetone (10:0.5 v/v)

E4: chloroform/acetone (10:1 v/v)

E5: butan-1-ol/acetic acid/water (3:1:1 by vol.)

Amino acid derivatives and peptides were visualized by one or more of the following procedures: ninhydrin, TDM reagent [3] and UV light. Sugar and sugar derivative-containing products were located by spraying the plates with 10% sulphuric acid in ethanol followed by heating for 10 min at 100 °C.

Low-pressure liquid chromatographies were performed on a Buchi 688 Chromatographic Pump (Silica Gel F 60, 230 × 49 mm column, flow rate 48 ml/min) connected with a Buchi UV/Vis Filter-Photometer Detector (254 nm) and a Knauer recorder; see text for elution conditions. Analytical HPLC separations were performed either on an Aquapore RP-300 column (220 × 4.6 mm, 7 μm, Brownlee Labs., flow rate 1.5 ml/min) or on a Delta-Pack C-18 column (150 × 3.9 mm, 5 μm, flow rate 1.0 ml/min, or 300 × 3.9 mm, 15 μm, flow rate 1.5 ml/min) in the indicated conditions, on a Perkin Elmer series 3B liquid chromatograph equipped with a LC-90 UV detector (230 nm) and LC-100 integrator. Eluents A (0.1% TFA in 90% aqueous acetonitrile) and B (0.1% aqueous TFA) were used for preparing binary gradients. Elution conditions for the Aquapore column: 1, isocratic 10% A for 2 min, linear gradient 10–30% A in 20 min and 30–90% A in 5 min; 2, isocratic 45% A for 2 min, linear gradient 45–80% A in 20 min and 80–100% A in 5 min. Elution conditions for the Delta-Pack columns: 3, isocratic 15% A for 2 min, linear gradient 15–50% A in 25 min and 50–90% A in 5 min; 4, isocratic 5% A for 2 min, linear gradient 5–30% A in 20 min and 30–90% A in 5 min. Solvents were dried and freshly distilled and evaporations were carried out under reduced pressure, at 40–50 °C, using a rotary evaporator. Yields are

based on the weight of vacuum-dried product. Magnesium sulphate was used for drying purposes.

Peptide Synthesis

The homo-oligomers of the series $\mathbf{I}_{1-4}$ and $\mathbf{II}_{1-5}$ were prepared by stepwise synthesis in solution starting, respectively, from H-Thr-$NHCH_3$ and H-[Gal-$(Ac)_4\beta$]Thr-$NHCH_3$, both obtained by catalytic hydrogenation of the corresponding N^{α}-benzyloxycarbonyl derivatives. The N^{α}-protected amino acid *N*-methyl amides were synthesized by reacting Z-Thr-OH, or Z-[Gal$(Ac)_4\beta$]Thr-OH, with HOBt-NH_2CH_3 in the presence of EDC as the coupling agent. During the synthesis the amino group of the growing peptide chain was deprotected by catalytic hydrogenation and the EDC-HOBt method was used for the activation of the carboxyl function of the C-component. Deacetylation of the carbohydrate moieties of the homo-oligomers of the $\mathbf{II}_{1-5}$ series by treatment with hydrazine in methanol yielded the corresponding glycopeptides of the $\mathbf{III}_{1-5}$ series. All synthesized peptides were homogeneous by TLC and analytical HPLC in the indicated conditions, and were characterized by optical rotation, proton NMR, IR spectroscopy and elemental analysis.

Z-Thr-NHCH$_3$, $\mathbf{I}_1$. HOBt-NH_2CH_3 (2.0 g, 12 mmol) and EDC (2.5 g, 13 mmol) were added to an ice-cooled solution of Z-Thr-OH (2.96 g, 11.7 mmol) in DMF (18 ml). The reaction mixture was stirred overnight, evaporated to dryness, and the residue taken up with 5% $NaHCO_3$ (80 ml) and extracted with AcOEt (3×50 ml). The organic layers were combined, washed with aqueous 5% $NaHCO_3$ (50 ml) and saturated NaCl (2×50 ml), dried and evaporated to dryness. Yield 2.74 g (88%); single spot by TLC in E1; m.p. 153–156 °C; $[\alpha]_D^{25} = -5.2°$ (c=0.76, MeOH); homogeneous by HPLC (elution conditions 1). Calculated for $C_{13}H_{18}O_4N_2$ (266.28): C 58.65; H 6.81; N 10.52. Found: C 58.70; H 6.84; N 10.23. Proton NMR data are shown in Table 1. Solution and solid-state IR data are shown in Tables 3 and 5, respectively.

Z-Thr-Thr-NHCH$_3$, $\mathbf{I}_2$. A solution of EDC (2.1 g, 11 mmol) in DCM/DMF (10 ml, 9:1 v/v) was added to an ice-cooled solution of Z-Thr-OH (2.53 g, 10 mmol) and HOBt (2.3 g, 17 mmol) in DCM/DMF (20 ml, 1:1 v/v). After 15 min a suspension of H-Thr-$NHCH_3$. HCl(1.69 g, 10 mmol) in DCM (20 ml) and Et_3N (1.4 ml, 10 mmol) were added [the amino component was separately prepared by catalytic hydrogenation of a methanolic solution of the Z-derivative

Table 1 NH Chemical Shifts (δ in p.p.m., TMS as the Internal Standard), NH-CH^{α} Coupling Constants (J in Hz) and Temperature Coefficients ($d\delta/dT$, in p.p.m. $\times 10^3$/K) in DMSO-d_6 Solution (Temperature Range 298–335 K) and in $CDCl_3$ (*) Solution (Temperature Range 298–320 K) of the Homo-oligomer Series **I, II** and **III**

	Terminal NH		Internal NH		NH-CH_3	
	δ NH ($^3J_{\alpha\text{-NH}}$)	$d\delta/dT$	δ NH ($^3J_{\alpha\text{-NH}}$)	$d\delta/dT$	δ NH ($^3J_{CHNH}$)	$d\delta/dT$
$\mathbf{I}_1$	6.84 (8.19)	−7.5			7.77 (4.4)	−5.4
$\mathbf{I}_2$	7.13 (8.5)	−7.0	7.64 (8.52)	−3.6	7.64 (4.7)	−4.8
$\mathbf{I}_3$	7.11 (8.58)	−6.9	7.83 (8.09); 7.62 (8.47)	−3.7; −4.0	7.59 (4.9)	−4.3
$\mathbf{I}_4$	7.12 (8.44)	−7.4	7.85 (7.85); 7.80 (7.94); 7.62 (8.62);	−3.7; −2.8; −3.3	7.60 (4.5)	−4.5
$\mathbf{II}_2$	6.90 (7.73)	−8.0	7.57 (8.0)	−4.2	7.44 (4.4)	−7.0
$\mathbf{II}_3$	6.91 (7.54)	−6.9	7.64 (7.8); 7.47 (7.82)	−4.0; −4.0;	7.29 (4.75)	−6.2
$\mathbf{II}_4$	6.93 (7.39)	−7.7	7.62 (7.5); 7.5 (7.6); 7.38 (–)	−4.0; −4.8; −3.3	7.23 (4.7)	−5.8
$\mathbf{II}_5$	6.91 (7.28)	−7.1	7.58 (7.0); 7.48 (7.41); 7.41 (6.98); 7.35 (–)	−3.7; −4.0; −3.3; −2.6	7.21 (4.5)	−6.0
$\mathbf{II}_1$*	5.93 (6.1)	−2.4			6.47 (4.2)	−2.7
$\mathbf{II}_2$*	5.84 (6.98)	−2.9	7.45 (6.6)	−2.0	6.47 (4.5)	−2.1
$\mathbf{II}_3$*	5.86 (6.45)	−2.7	7.43 (6.8); 7.31 (6.91)	−2.6; −1.8	6.47 (4.5)	−1.8
$\mathbf{II}_4$*	5.88 (6.07)	−3.3	7.4 (7.28); 7.34 (6.63); 7.27 (5.67)	−2.9; −2.0; −1.5	6.48 (4.67)	−1.8
$\mathbf{II}_5$*	5.88 (6.08)	−3.5	7.38(–); 7.35 (–); 7.27 (–) 7.26 (–)	−2.6; −1.4; −1.4; −1.6	6.49 (4.84)	−1.9
$\mathbf{III}_1$	6.94 (7.97)	−7.8			7.68 (4.19)	−5.0
$\mathbf{III}_2$	7.30 (7.78)	−7.6	7.59 (7.51)	−2.6	7.39 (4.95)	−3.0
$\mathbf{III}_3$	7.30 (7.78)	−7.4	7.73 (7.57); 7.63 (7.68)	−3.3 −2.4	7.43 (4.37)	−3.0
$\mathbf{III}_4$	7.30 (–)	−7.5	7.77 (7.64); 7.70 (7.46); 7.65 (7.17)	−3.8; −2.4; −2.2	7.49 (4.58)	−3.6
$\mathbf{III}_5$	7.30 (–)	−7.9	7.74 (–); 7.74 (–); 7.74 (–); 7.65 (7.17)	−2.0; −2.0; −2.0; −2.2	7.43 (4.78)	−2.9

and precipitated with 4N HCl in dioxane (yield 95%]. After 4 h stirring the solvent was removed and the oily residue taken up with AcOEt (80 ml) and worked up as described for $\mathbf{I}_1$. Yield 3.2 g (87%); single spot by TLC in E1; m.p. 175–176 °C; $[\alpha]_D^{25} = -13.9°$ (c=1.1, MeOH); homogeneous by HPLC (elution conditions 1). Calculated for $C_{17}H_{25}O_6N_3$ (367.41): C 55.57; H 6.87; N 11.44. Found: C 56.12; H 6.94; N 11.30. For the ^{1}H-NMR data see Table 1 and for the IR data see Tables 3 and 5.

Z-Thr-Thr-Thr-NHCH$_3$, **$\mathbf{I}_3$**. The title compound was prepared from Z-Thr-OH (1.82 g, 7.1 mmol), HOBt (1.65 g, 12.2 mmol), EDC (1.51 g, 7.9 mmol), H-Thr-Thr-NHCH$_3$. HCl (1.94 g, 7.2 mmol) and Et$_3$N (2 ml, 14.4 mmol) in DCM/DMF (20 ml, 1:1 v/v) as described for $\mathbf{I}_2$. Reaction time 22 h. Yield 1.69 g (50%); single spot by TLC in E1; m.p. 196–197 °C; $[\alpha]_D^{25} = -23°$ (c=0.85, MeOH); homogeneous by HPLC (elution conditions 1). Calculated for $C_{21}H_{32}O_8N_4$ (468.52): C 53.83; H 6.88; N 11.96. Found: C 52.44; H 6.86; N 11.86. For the ^{1}H-NMR data see Table 1 and for the IR data see Tables 3 and 5.

Z-Thr-Thr-Thr-Thr-NHCH$_3$, **$\mathbf{I}_4$**. Prepared from Z-Thr-OH (0.527 g, 2.08 mmol), HOBt (0.477 g, 3.5 mmol), DC (0.426 g, 2.22 mmol), H-Thr-Thr-Thr-NHCH$_3$. HCl (0.696 g, 2.08 mmol) and Et$_3$N (0.51 ml, 3.66 mmol) as described for $\mathbf{I}_2$. Reaction time 20 h. Yield 0.5 g (42%); single spot by TLC in E2; m.p. 173–175 °C; $[\alpha]_D^{25} = -40.3°$ (c=0.79, water); homogeneous by HPLC (elution conditions 1). Calculated for $C_{25}H_{39}O_{10}N_5$ (569.61): C 52.72; H 6.90; N 12.29. Found: C 52.28; H 6.77; N 12.06. For the ^{1}H-NMR data see Table 1 and for the IR data see Table 5.

Z-(Gal(Ac)$_4$ β)Thr-OH. Z-OSu (1.1 g, 4.45 mmol) and Et$_3$N (0.62 ml, 4.45 mmol) were dissolved in acetonitrile (25 ml) and added to an ice-cooled solution of H-[Gal(Ac)$_4\beta$]Thr-OH [4] (2.0 g, 4.45 mmol) in water (30 ml). After 30 min at room temperature the organic solvent was removed, the aqueous solution acidified to pH 6 by adding solid KHSO$_4$, and extracted with ethyl acetate (3 × 10 ml). The organic phases were combined, washed with water (3 × 20 ml), dried and evaporated *in vacuo*. Yield 2.5 g (96%); single spot by TLC in E1; m.p. 55–59 °C; $[\alpha]_D^{25} = +2.1°$ (c=1.14, MeOH). Calculated for $C_{26}H_{33}O_{14}N$ (583.19): C 53.52; H 5.70; N 2.40. Found: C 53.94; H 5.83; N 2.55. IR (KBr) ν_{max} 3432, 1748, 1515. ^{1}H-NMR (200 MHz, CDCl$_3$): 7.37 (m, 5H, phenyl); 5.61 (d, 1H, CONH, $^3J_{\alpha,\,NH}$ 8.9 Hz); 5.37 (m, 1H, H-4); 5.12 (dd, 1H, H-2); 5.11 (s, 2H, CH$_2$); 4.98 (dd, 1H, H-3); 4.51 (d, 1H, H-1, $^3J_{1,2}$ 7.7 Hz); 4.43 (m, 1H, β-CH); 4.37 (m, 1H, α-CH); 4.15 (m, 2H, H-6, H-6′); 3.84 (dd, 1H, H-5); 2.14, 2.04, 1.98 (m, 12H, 4 CH$_3$CO); 1.23 (d, 3H, γ-CH$_3$).

Z-(Gal(Ac)$_4$ β)Thr-NHCH$_3$, **$\mathbf{II}_1$**. EDC (1.7 g, 9.0 mmol) was added to an ice-cooled solution of Z-[Gal-(Ac)$_4\beta$]Thr-OH (4.7 g, 8.0 mmol) and HOBt-NH$_2$CH$_3$ (1.3 g, 8.0 mmol) in anhydrous DMF (20 ml). After 3 h stirring, the reaction mixture was evaporated to dryness and the residue taken up with ethyl acetate (120 ml), washed with 5% NaHCO$_3$ (2 × 60 ml), 0.1N KHSO$_4$ (2 × 60 ml) and saturated aqueous NaCl, dried and evaporated to dryness. Yield 4.3 g (90%); single spot by TLC in E4; m.p. 121–123 °C; $[\alpha]_D^{25} = +1.9°$ (c=0.25, MeOH); homogeneous by HPLC (elution conditions 2). Calculated for $C_{27}H_{36}O_{13}N_2$ (596.54); C 54.36; H 6.03; N 4.69. Found: C 54.52; H 6.02; N 4.70. For the ^{1}H-NMR data see Table 1 and for the IR data see Tables 4 and 5.

H-(Gal(Ac)$_4$ β)Thr-NHCH$_3$. Z-[Gal(Ac)$_4\beta$]Thr-NHCH$_3$ (4.28 g, 7.17 mmol) was dissolved in methanol (40 ml) and hydrogenated in the presence of 10% Pd/C. After 60 min the catalyst was removed by filtration, the solution evaporated to dryness and the oily residue dissolved in diethyl ether and precipitated with 4N HCl in dioxane. The crude product was dissolved in water (50 ml), the pH value adjusted to 8 with 5% NaHCO$_3$, and the solution extracted with ethyl acetate (2 × 20 ml). The combined organic layers were dried and evaporated to dryness. Yield 2.62 g (79%); single spot by TLC in E1; oil; $[\alpha]_D^{25} = -7.6°$ (c=0.87, Me OH). Calculated for $C_{19}H_{29}O_{11}N_2$ (461.44): C 49.45; H 6.33; N 6.07. Found: C 49.65; H 6.53; N 5.68. IR (KBr) ν_{max} 3403, 1749, 1667, 1534. ^{1}H-NMR (200 MHz, CDCl$_3$): 7.15 (broad, 1H, N*H*-CH$_3$); 5.4 (dd, 1H, H-4); 5.15 (dd, 1H, H-2); 5.0 (dd, 1H, H-3); 4.5 (d, 1H, H-1, $^3J_{1,2}$ 7.7 Hz); 4.25 (m, 1H, β-CH); 4.1 (d, 2H, H-6, H-6′); 3.85 (td, 1H, H-5); 3.25 (m, 1H, α-CH); 2.8 (d, 3H, NH–C*H*$_3$, $^3J_{CH\text{-}NH}$ 4.9 Hz); 2.2, 1.95 (4s, 12H, 4 CH$_3$CO); 1.15 (d, 3H, γ-CH$_3$).

Z-{(Gal(Ac)$_4$ β)Thr}$_2$-NHCH$_3$, **$\mathbf{II}_2$**. Prepared from Z-[Gal-(Ac)$_4\beta$]Thr-OH (2.8 g, 4.79 mmol), HOBt (1.1 g, 8.1 mmol), EDC (1.0 g, 5.2 mmol), and H-[Gal-(Ac)$_4\beta$]Thr-NHCH$_3$ (2.2 g, 4.8 mmol in 13 ml of DCM) in DCM/DMF (10 ml, 1:1 v/v) as described for the preparation of $\mathbf{II}_1$. Reaction time 2 h. Yield

4.51 g (92%); single spot by TLC in E1; m.p. 110–112 °C; $[\alpha]_D^{25} = +1.5°$ (c=1.2, MeOH); homogen-eous by HPLC (elution conditions 2). Calculated for $C_{45}H_{61}O_{24}N_3$ (1027.99): C 52.57; H 5.98; N 4.08. Found: C 52.60; H 5.93; N 3.95. For the ^{1}H-NMR data see Table 1 and for the IR data see Tables 4 and 5.

***Z-{(Gal(Ac)$_4$ β)Thr}$_3$-NHCH$_3$,* $\mathbf{II_3}$**. Prepared from Z-[Gal-(Ac)$_4\beta$]Thr-OH (2.3 g, 3.9 mmol), HOBt (0.9 g, 6.6 mmol), EDC (0.8 g, 4.3 mmol), and H-{[Gal-(Ac)$_4\beta$]Thr}$_2$-NHCH$_3$ (3.5 g, 3.9 mmol) as described for $\mathbf{II}_1$. Reaction time 2 h. Yield 4.46 g (78%); single spot by TLC in E1; m.p. 156–158 °C; $[\alpha]_D^{25} = +3.9°$ (c=1.23, MeOH); homogeneous by HPLC (elution conditions 2). Calculated for $C_{63}H_{86}O_{35}N_4$ (1459.39): C 51.85; H 5.94; N 3.84. Found: C 51.88; H 5.92; N 3.77. For the ^{1}H-NMR data see Table 1 and for the IR data see Tables 4 and 5.

***Z-{(Gal(Ac)$_4$ β)Thr}$_4$-NHCH$_3$,* $\mathbf{II_4}$** Prepared from Z-[Gal-(Ac)$_4\beta$]Thr-OH (1.32 g, 2.26 mmol), HOBt (0.52 g, 3.85 mmol), EDC (0.48 g, 2.5 mmol), and H-{[Gal(Ac)$_4\beta$Thr}$_3$-NHCH$_3$ (3.0 g, 2.26 mmol) as described for $\mathbf{II}_1$. Reaction time 4 h. In this case a further purification was needed and the product was taken up once more in ethyl acetate (50 ml), extracted with 0.1N $KHSO_4$ (2 × 30 ml), dried and evaporated to dryness. Yield 2.94 g (69%); single spot by TLC in E1; m.p. 134–135 °C; $[\alpha]_D^{25} = +4.82°$ (c=0.83, MeOH); homogeneous by HPLC (elution conditions 2). Calculated for $C_{81}H_{111}O_{46}N_5$ (1890): C 51.45; H 5.92; N 3.70. Found: C 50.34; H 5.74; N 3.47. See Table 1 for the ^{1}H-NMR data and Tables 4 and 5 for the IR data.

***Z-{(Gal(Ac)$_4$ β)Thr}$_5$-NHCH$_3$,* $\mathbf{II_5}$**. Prepared from Z-[Gal(Ac)$_4\beta$]Thr-OH (0.46 g, 0.79 mmol), HOBt (0.18 g, 1.34 mmol), EDC (0.17 g, 0.91 mmol) and H-{[Gal(Ac)$_4\beta$]Thr}$_4$-NHCH$_3$ (1.38 g, 0.79 mmol) and isolated as described for $\mathbf{II}_1$. The product, still inhomogeneous by TLC in E1, was further purified by medium-pressure liquid chromatography (3.5% methanol in chloroform as the eluent). Fractions containing the pure product (TLC in E1) were combined, evaporated to dryness and the residue was triturated with *tert*-butyl methyl ether and dried. Yield 0.53 g (29%); m.p. 136–138 °C; $[\alpha]_D^{25} = +4.3°$ (c=0.98, MeOH); homogeneous by HPLC (elution conditions 2). Calculated for $C_{99}H_{136}O_{57}N_6$ (2322): C 51.20; H 5.90; N 3.62. Found: C 51.03; H 5.89; N 3.45. See Table 1 for the ^{1}H-NMR data and Tables 4 and 5 for the IR data.

Deacetylation Procedure

All the homo-oligomers of the series $\mathbf{II}_{1-5}$ were deacetylated with hydrazine hydrate using the same procedure. All the resulting homo-oligomers of the series $\mathbf{III}_{1-5}$ were homogeneous by TLC (E1, E5) and HPLC (elution conditions 3 for $\mathbf{III}_{1-3}$ and 4 for $\mathbf{III}_4$ and $\mathbf{III}_5$), and gave the expected elemental analyses (C, H, N). For the ^{1}H-NMR data see Table 1 and for the IR data see Table 5. As an example, the deacetylation of Z-[(Gal(Ac)$_4\beta$]Thr-NHCH$_3$ is described in detail. Yields and analytical data are shown in Table 2.

***Z-(Galβ)Thr-NHCH$_3$* $\mathbf{III_1}$**. Hydrazine hydrate (0.64 ml, 13.2 mmol) was added to a solution of $\mathbf{II}_1$ (393 mg, 0.66 mmol) in MeOH (10 ml) and the reaction was monitored by TLC (E1). After 3 h the mixture was cooled in an ice-bath and 2,4–pentanedione (1.36 ml, 13.2 mmol) was added. After further 60 min the solution was evaporated to dryness and the residue taken up with water (100 ml) and extracted with chloroform (6 × 40 ml). The aqueous phase was first concentrated to a small volume and then lyophilized. The product was precipitated from MeOH with diethyl ether and triturated with *tert*-butyl methyl ether.

Methyl 2,3,4,6-tetra-*O*-acetyl-β-D-galactopyranoside

The title compound was prepared for establishing the contribution of the tetra-acetylated sugar moiety to the CD spectra. Acetic anhydride (7.6 ml, 80 mmol) and DMAP (0.2 g, 1.6 mmol) were added under stirring to an ice-cooled solution of methyl β-D-galactopyranoside (2.0 g, 10 mmol) in pyridine (5 ml). The mixture was stirred overnight at room temperature and the solvent was removed *in vacuo*. The oily residue was dissolved in ethyl acetate (100 ml), washed with water (1 × 30 ml), 0.1 M $KHSO_4$ (2 × 30 ml), 5% $NaHCO_3$ (1 × 30 ml), saturated NaCl aqueous solution, dried and evaporated

Table 2 Yields and Analytical Data of the Indicated Homo-oligomers of the Series **III**

Oligomer	Yield (%)	M.p. (°C)	$[\alpha]_D^{25}$	(H_2O)
$\mathbf{III}_1$	38	118–119	+0.66°	(c=0.90)
$\mathbf{III}_2$	59	167–169	−1.42°	(c=0.91)
$\mathbf{III}_3$	93	184–186	−4.42°	(c=0.81)
$\mathbf{III}_4$	98	197–198	−6.94°	(c=0.86)
$\mathbf{III}_5$	98	205–206	−6.28°	(c=0.86)

to dryness. Crystallization from ethanol of the oily residue gave 1.9 g (52%); m.p. 93–94 °C; $[\alpha]^{25}_{D}=-13.9°$ (c=2.65, $CHCl_3$); single spot by TLC in E1. Calculated for $C_{15}H_{22}O_{10}$ (362.33): C 49.72; H 6.12. Found: C 50.46; H 6.01. IR (KBr): ν_{max} 3479, 1751. ^{1}H-NMR (400 MHz, $CDCl_3$): 5.39 (q, 1H, H-4, $^3J_{4,3}$ 3.47 Hz, $^3J_{4,5}$ 1.0 Hz); 5.19 (q, 1H, H-2, $^3J_{2,3}$ 10.5 Hz, $^3J_{2,1}$ 7.9 Hz); 5.01 (dd, 1H, H-3, $^3J_{3,2}$ 10.5 Hz, $^3J_{3,4}$ 3.47 Hz); 4.4 (d, 1H, H-1, $^3J_{1,2}$ 7.84); 4.20 (dd, 1H, H-6, $^3J_{6,5}$ 6.49 Hz, $^3J_{6,6'}$ 11.21 Hz); 4.13 (dd, 1H, H-6′, $^3J_{6',5}$ 6.98 Hz); 3.9 (m, 1H, H-5); 3.51 (s, 3H, OCH_3); 2.15 (s, 3H, CH_3CO); 2.06 (s, 3H, CH_3CO); 2.05 (s, 3H, CH_3CO); 1.98 (s, 3H, CH_3CO).

Infrared Absorption

Infrared absorption spectra were recorded with a Perkin Elmer Model 1720 FT-IR spectrophotometer (Norwalk, Connecticut, USA), nitrogen flushed, at 2 cm^{-1} nominal resolution, average 16 scans for 10 and 1.0 mM sample concentrations, or 64 scans for 0.1 mM sample concentration. Solvent (baseline) spectra were recorded under the same conditions. Cells with path lengths of 0.1, 1.0 and 10 mm (with CaF_2 windows) were used. Spectrograde deuterochloroform (99.8% d) was purchased from Merck (Darmstadt, Germany). For the solid-state measurements a Perkin-Elmer 580 B infrared spectrophotometer, with a Perkin Elmer infrared data station, and the KBr disk technique were used. Elaboration of the spectra with subtraction of the baseline and the second derivative was carried out with a Spectra Calc. program (Galactic, Salem, USA).

Proton Nuclear Magnetic Resonance

Proton NMR spectra were recorded with a Bruker AC-200, a Bruker Ac-250F or a Bruker Model AM-400 spectrometer. Measurements were carried out at 298 K in $CDCl_3$ (99.96%) d, Merck) and DMSO-d_6 (99.96% d_6, Fluka, Buchs, Switzerland) with tetramethylsilane as the internal standard. Sample concentration was in the range 8–10 mg/ml. The free radical TEMPO was purchased from Sigma (St. Louis, Missouri, USA). Spectra at different temperatures were only recorded at 400 MHz, at a sample concentration of 5 mg/0.5 ml. NMR spectra of all the homo-oligomers of the three series were fully consistent with their structures.

Circular Dichroism

CD measurements were performed at 298 K, over the 250–190 nm region, using either a Jasco-600 or a Jasco-715 spectropolarimeter. The number of accumulated scans ranged from 4 to 8, depending on the intensity of the CD signal. Sample concentration was about 1 mM in water and in TFE and the optical path length was 0.02 cm. The spectra reported are original computer-drawn CD curves. The limited contribution of the acetylated, or deacetylated, sugar moieties to the optical activity of the different homo-peptides was subtracted from the oligomer spectra; $[\theta]_R$ represents the residue molar ellipticity (deg cm^2/dmol).

RESULTS AND DISCUSSION

Infrared Absorption

The conformational preferences of the homo-oligomers of the three series were examined by FT-IR absorption in a structure-supporting solvent ($CDCl_3$, peptide concentrations in the range 10–0.1 mM) and in the solid state (KBr pellets). As pointed out above, only IR solid-state measurements were possible for $\mathbf{I}_4$ and the entire $\mathbf{III}_{1-5}$ series. The infrared absorption frequencies of the oligomers $\mathbf{I}_{1-3}$ and $\mathbf{II}_{1-5}$ in the 3500–3250 cm^{-1} region (N-H stretching mode) and 1800–1600 cm^{-1} region (C=O stretching mode), as obtained from the second derivative spectra, in $CDCl_3$ solution at different concentrations are shown in Tables 3 and 4, respectively. For comparison the absorption frequencies determined for the homo-polymer poly-{[Gal(Ac)$_4$ β]Thr} (MW $\approx$ 80,000) [1] are also reported in Table 4. The infrared absorption frequencies of the three series in the solid state are shown in Table 5 together with those of poly-{[Gal(Ac)$_4\beta$]Thr} and poly-[(Galβ)Thr] [1].

The FT-IR absorption spectra, in the 3500–3250 cm^{-1} region, of all the members of the $\mathbf{II}_{1-5}$ series (peptide concentration 1.0 mM) are shown in Figure 1. The spectrum of the monomer $\mathbf{II}_1$ exhibits an intense band at 3413 cm^{-1} (very weakly H-bonded NH groups), a shoulder at 3450 cm^{-1} (free NH groups) and a weak, broad band at about 3490 cm^{-1}. In the dipeptide $\mathbf{II}_2$ spectrum a new absorption is visible at about 3330 cm^{-1}, while the shoulder at 3450 cm^{-1} disappears. The intensities of the 3413 and 3330 cm^{-1} bands gradually increase with increasing main-chain length. Concomitantly, the absorption at 3330 cm^{-1} shifts towards higher

Table 3 Infrared Absorption Frequencies (cm^{-1}) of the Indicated Oligomers in $CDCl_3$ Solution

Oligomer	Conc. (mM)	IR frequencies (ν_{max})							
I_1	10	3426s		1708s		1669s		1538m	1501s
	1.0	3426s		1707s		1669s		1539m	1501s
	0.1	3426s							
I_2	1.0	3417s		1717m		1669s		1540sh	1499m
	0.1	3415s							
I_3	1.0	3416w	3287s		1687m	1655w	1616s	1555m	1500w
	0.1	3417w	3289m						

s, strong; m, medium; w, weak; sh, shoulder.

Table 4 Infrared Absorption Frequencies (cm^{-1}) of the Indicated Oligomers in $CDCl_3$ Solution

Oligomer	Conc. (mM)	IR frequencies (ν_{max})							
II_1	10	3500w	3413s		1750s	1715 sh		1677m	1498m
	1.0	3490w	3413s		1750s	1715 sh		1677m	1498m
	0.1		3412s						
II_2	10	3500w	3415s	3330w	1751s	1715 sh	1680 sh	1666w	1495w
	1.0	3500w	3414s	3330w	1751s	1715 sh	1680 sh	1660w	1492w
	0.1		3413s	3330w					
II_3	10	3490w	3412s	3360m	1751s		1691w	1662w	1492w
	1.0	3490w	3411s	3360m	1751s	1715 sh	1692w	1664w	
	0.1	3480w	3411s	3360m					
II_4	10	3490w	3407s	3370s	1751s		1693w	1663w	1498w
	1.0	3480w	3405s	3370s	1751s		1693w	1663w	1495w
	0.1	3480w	3405s	3370s					
II_5	10	3490w		3380s					
	1.0	3480w		3380s	1753s		1695w	1662w	1489w
	0.1	3480w	3405w	3380s					
poly II[a]		3480w		3368s	1752s		1696w	1663w	

s, strong; m, medium; w, weak; sh, shoulder; [a]Poly-II is poly-{[Gal(Ac)$_4\beta$]Thr} (MW $\approx$80,000); ref. [1].

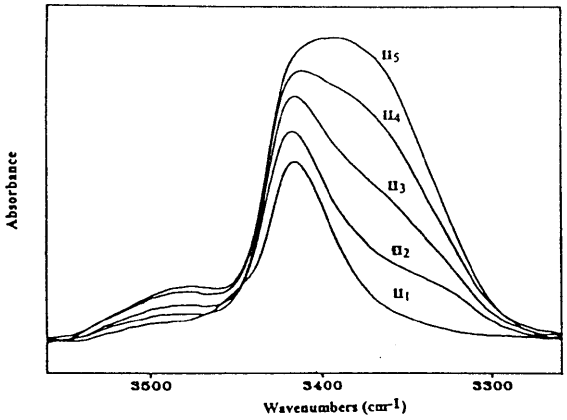

Figure 1 FT-IR absorption spectra in the N–H stretching region of the Z-{[Gal(Ac)$_4\beta$]Thr}$_{1-5}$-$NHCH_3$ homo-peptides (**II_{1-5}**) in $COCl_3$ solution (concentration 1.0 mM).

wavenumbers and in **II_5** the two bands overlap in a broad absorption maximum centred at about 3380 cm^{-1}. In the concentration range examined (1.0–0.1 mM) the FT-IR absorption spectra of the oligomers **II_{1-5}** remain substantially unchanged, suggesting that no self-association through intermolecular H-bonding occurred. The IR absorption results provide evidence that intramolecular NH$\cdots$O=C interactions predominate in the conformational equilibrium mixtures of the homo-oligomers of the **II_{1-5}** series in $CDCl_3$ solution. The presence of bands between 3415 and 3400 cm^{-1} may be ascribed to the existence of structures stabilized by five-atom hydrogen-bonded rings in which the molecules accommodate the extended conformation C_5 [5–7]. The bands between 3330 and 3400 cm^{-1} have often been assigned to the γ-turn (C_7) conformation [5, 8–10].

Table 5 Infrared Absorption Frequencies (cm^{-1}) of the Indicated Oligomers in the Solid State (KBr pellets)

Oligomer	IR frequencies (υ_{max})					
I_1	3378m	3299s		1691s	1633s	1520s
I_2	3400 sh	3285s		1693s	1640s	1537m
I_3	3400 sh	3297s		1690 sh	1642s	1541m
I_4		3369s			1651s	1526m
II_1	3450 sh	3405m	1748s	1700 sh	1673m	1500m
II_2	3500 sh	3411m	1749s	1700 sh	1669m	1505m
II_3	3500 sh	3407m	1750s		1667m	1505m
II_4	3500 sh	3403m	1750s		1666m	1503m
II_5	3500 sh	3399m	1751s		1665m	1501m
Poly II[a]		3389m	1752s		1663m	1494m
III_1		3407s		1709m	1657m	1535m
III_2		3388s		1700 sh	1656m	1527m
III_3		3386s		1700 sh	1653s	1522m
III_4		3387s			1650s	1521m
III_5		3387s			1650s	1521m
Poly III[b]		3385s			1648s	1521m

s, strong; m, medium; w, weak; sh, shoulder.
[a]Poly-{[Gal(Ac)$_4\beta$]Thr} (MW≈80,000); ref. [1].
[b]Poly-[(Galβ)Thr] (MW≈50,000); ref. [1].

A population of C_7 structures is consistent with the intramolecularly H-bonded peak at 3380 cm^{-1} of the $\mathbf{II}_4$ and $\mathbf{II}_5$ oligomers. In the $\mathbf{II}_2$ and $\mathbf{II}_3$ derivatives the low-frequency band at about 3330 cm^{-1} may also suggest the presence of a H-bonded β-turn [9, 10], but the C=O stretching vibration does not support this structure [11, 12]. In the 1800–1600 cm^{-1} region (Table 4) the different kinds of C=O groups give rise to three main different bands. The ester C=O groups are non-H-bonded and show absorption maxima at 1753–1750 cm^{-1}. The urethane C=O group gives a band at 1715 cm^{-1} (shoulder), whose intensity decreases form $\mathbf{II}_1$ to $\mathbf{II}_3$, while, starting from $\mathbf{II}_2$, a new absorption, increasing with peptide chain elongation, is visible at 1680–1696 cm^{-1}. The shift to lower frequencies suggests the involvement of the urethane C=O group in intramolecular hydrogen bonding [10]. The amide I band of the monomer appears at 1677 cm^{-1}, shifts to 1660 cm^{-1} in the dimer, and its position practically remains unchanged up to the pentamer. This finding seems to indicate that an intra molecularly H-bonded structure is formed at the dimer level [11], the frequency values being consistent with weakly H-bonded N–H and C=O groups. The poly-{[Gal(Ac)$_4\beta$]Thr} [1] spectrum is quite similar to those of the homo-peptide $\mathbf{II}_5$. A comparison between the IR data obtained in solution (Table 4) and in the solid state (Table 5) for the oligomers $\mathbf{II}_{1-5}$ suggests that the intramolecular interactions are similar.

The structure of the deacetylated derivatives $\mathbf{III}_{1-5}$ in the solid state is characterized by the presence of NH and C=O groups which are bonded more strongly than in the corresponding derivatives $\mathbf{II}_{1-5}$. As for the type of secondary structure formed, the positions of the amide I band (1648–1657 cm^{-1}) and amide **II** band (1521–1535 cm^{-1}) are not compatible with the onset of a β-sheet structure [12]. The solid-state IR absorption spectra of the homo-peptide $\mathbf{III}_5$ is similar to those of the poly-[(Galβ)Thr] [1].

The oligomers $\mathbf{I}_1$ and $\mathbf{I}_2$ in $CDCl_3$ solution show a maximum at 3426–3415 cm^{-1} (Table 3) which is indicative of either free or extremely weakly H-bonded NH groups. In the IR spectrum of $\mathbf{I}_3$, at 1.0 mM concentration, an intense band, related to strongly H-bonded NH groups, is visible at 3287 cm^{-1}. This band, whose intensity decreases at 0.1 mM concentration, may be assigned to intermolecularly hydrogen-bonded species. The presence of strong hydrogen bonds would be expected to produce a corresponding amide I maximum shifted to significantly low frequencies. Indeed an intense feature is observed at 1616 cm^{-1}. The IR spectra of the oligomers of the $\mathbf{I}_{1-4}$ series in the solid state (Table 5) make evident their tendency to self-associate.

Proton Nuclear Magnetic Resonance

Additional information on the conformational preferences of the Thr-based terminally protected homo-oligomers can be drawn from the NMR experiments. The ^{1}H-NMR parameters for the NH resonances in the oligomers of the three series are summarized in Table 1. Chemical shifts, NH–CH$^\alpha$ coupling constants and temperature coefficients [13, 14] were determined in DMSO-d_6 for the $\mathbf{I}_{1-4}$ and $\mathbf{III}_{1-5}$ series and in DMSO-d_6 and $CDCl_3$ for the $\mathbf{II}_{2-5}$ series. In both solvents, $CDCl_3$ and DMSO-d_6, the NH resonance of the N-terminal residue (Thr^1) of all the homopeptides, owing to the presence of the urethane protecting group, is considerably shifted upfield from the remaining NH signals which arise from an NH involved in a peptide bond [15, 16]. The signal of the C-terminal $NHCH_3$ at lower fields is identified by its multiplicity. The NH resonance of Thr^2 in the dipeptides is assigned by elimination. An unequivocal assignment of the internal NH signals for the tri-, tetra- and pentapeptides is not possible. The resonances reported in Table 1 for the internal NH protons are arbitrarily listed in a decreasing order. Obviously, with increasing peptide main-chain length, the number of NH proton doublets increases and their occurrence in a narrow range of chemical shifts may be considered as a first indication of a closely related structural environment for all internal NH groups, particularly in the higher member of the series, and represents a preliminary indication of the involvement of these protons in a H-bonding scheme [11, 14].

In the weakly interacting medium $CDCl_3$, both main-chain elongation and temperature variation induce remarkably small effects in the NH chemical shifts of the $\mathbf{II}_{1-5}$ oligomers (Table 1). As a representative example, the variations of the NH chemical shifts vs. temperature for $\mathbf{II}_4$ are illustrated in Figure 2 (A). In the range of temperature examined, the chemical shift variations are linear and negligible and the coupling constant changes are limited, suggesting that no major conformational rearrangement occurred [17]. The low-temperature coefficients indicate that initially the NH protons are either exposed to the solvent or shielded (hydrogen bonded or buried) and that their environment remains unchanged through the temperature range examined. [15, 16, 18]. The solvent accessibility of the NH protons, which is indicative of a possible participation to hydrogen bonds, was examined by adding increasing amounts either of DMSO-d_6 [19, 20] or of the paramagnetic radical TEMPO [21] to the $CDCl_3$ solution. As an example, the effect of the perturbing agent DMSO-d_6 on the chemical shifts of the NH protons of $\mathbf{II}_4$ is shown in Figure 2(B). The solvent titration curves provide no clear evidence for solvent-dependent conformational transitions up to a 20% concentration of DMSO-d_6. The NH protons of $\mathbf{II}_{3-5}$ are slightly sensitive to the perturbing agent and very probably highly shielded from the solvent. Only the Thr^1 NH resonance is perturbed, although

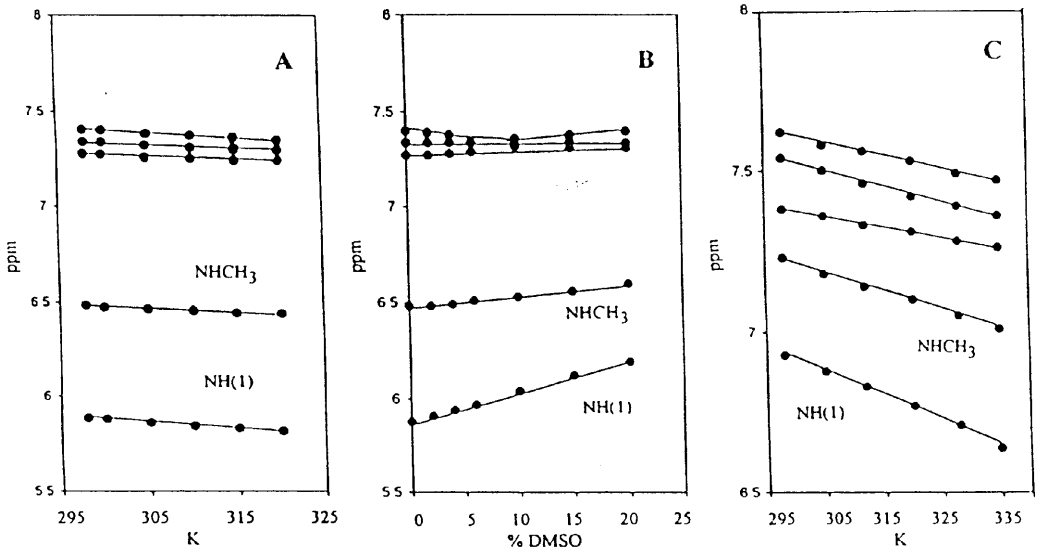

Figure 2 Plot of NH chemical shifts in ^{1}H-NMR spectrum of Z-{Gal(Ac)$_4\beta$]Thr}$_4$-$NHCH_3$ ($\mathbf{II}_4$):(A) vs. temperature in $CDCl_3$ solution; (B) as a function of increasing percentages of DMSO-d_6 to the $CDCl_3$ solution (v/v); (C) vs. temperature in DMSO-d_6 solution.

to a minor extent, by DMSO-d_6, suggesting a partial solvent exposure. Similar conclusions can be drawn from the results (not shown) of the paramagnetic radical-induced line-broadening study. These NMR findings seem to indicate that, in a solvent of low polarity, intramolecularly hydrogen-bonded forms (C_5 and γ-turns) significantly populate the conformational equilibrium mixtures of the glycosylated and acetylated homo-peptides, and confirm the FT-IR absorption results discussed above. On going from the poor hydrogen-bonding solvent $CDCl_3$ to a strongly hydrogen-bond accepting solvent such as DMSO-d_6, the Thr^1 NH and $NHCH_3$ amide protons of the series $\mathbf{II}_{2-5}$ show relatively large downfield shifts (1.0 p.p.m. and 0.97–0.72 p.p.m., respectively) and high temperature coefficients (Table 1), suggesting that these groups are fully exposed to the solvent. The central part of the peptide sequences seems to be less accessible to the solvent as the internal NH protons exhibit small changes in their chemical shifts (0.21–0.09 p.p.m.). In the oligomers $\mathbf{II}_4$ and $\mathbf{II}_5$ one and two NH groups, respectively, give intermediate temperature coefficients (0.0037–0.0033 p.p.m./K), suggestive of a partial shielding and of weak hydrogen bonds, while one NH proton exhibits a low $d\delta/dT$ value (0.002 p.p.m./K), characteristic of a solvent-shielded and intramolecularly hydrogen-bonded NH group. The variations of the NH chemical shifts vs. temperature, in DMSO-d_6, for $\mathbf{II}_4$ are shown in Figure 2(C). The changes in the chemical shifts are linear in the temperature range examined, suggesting that no major conformational rearrangements occurred. The $^3J_{\alpha\text{-NH}}$ values, on average larger than those determined in $CDCl_3$, may indicate a more extended conformation: it seems that in DMSO-d_6 the peptide overall structure only suffers small rearrangements, mainly involving hydrogen-bonding interactions of the terminal residues. In the $\mathbf{II}_4$ and $\mathbf{II}_5$ members of the series folded forms similar to those determined in $CDCl_3$ (γ conformations) may exist in equilibrium with partially unfolded structures.

In the deacetylated oligomers $\mathbf{III}_{1-4}$, in DMSO-d_6 solution, the signals of the NH protons are completely resolved but in the pentamer $\mathbf{III}_5$ the three NH doublets partially overlap. The Thr^1 NH proton temperature coefficients are high (0.0074–0.0079 p.p.m./K) for the entire $\mathbf{III}_{1-5}$ series, while those for $NH–CH_3$ decrease to intermediate values on going from the monomer to the pentamer (0.005 p.p.m./K for $\mathbf{III}_1$ and 0.0036–0.0029 p.p.m./K for $\mathbf{III}_{2-5}$). Internal amide protons $d\delta/dT$ values, particularly those of $\mathbf{III}_5$ (0.002–0.0022 p.p.m./K), are characteristic of solvent-shielded NH groups. The low coefficients probably reflect stronger hydrogen bonds in the deacetylated derivatives than in the corresponding acetylated ones. Moreover, in the higher oligomers of the series **III** also the $NH–CH_3$ residue may be involved in an intramolecular hydrogen bond. The $^3J_{\alpha\text{-NH}}$ values may suggest an extended conformation and the linear chemical shift variations indicate that no major conformational rearrangements occurred in the temperature range examined. The NH chemical shifts of $\mathbf{III}_5$, virtually identical, could indicate a disordered form [16] for this peptide, but the five α-CH protons give rise to a signal pattern 1:2:1:1 (not shown) that might suggest the formation of a preferred conformation, stabilized by hydrogen bonds [22]. The involvement (starting from Thr^2) of the NH protons in intramolecular hydrogen bonds might suggest the presence of a γ-turn conformation. On the other hand, the peptide backbone conformation could be also induced by an interaction with the bulky galactosyl side-chain residues. the downfield shift of the amide protons occurring in all of the $\mathbf{III}_{1-5}$ oligomers, when compared with the acetylated derivatives, may be due to the steric limitation of the spatial arrangements of the bulky side chains [22].

In the peptides $\mathbf{I}_{1-4}$, the Thr^1 NH and $NH–CH_3$ groups appear to be exposed to DMSO-d_6 in which they exhibit large temperature coefficients (0.0069–0.0075 and 0.0043–0.0054 p.p.m./K, respectively). The low $d\delta/dT$ value (0.0028 p.p.m./K) of one of the internal amide groups of $\mathbf{I}_4$ could suggest the presence of a hydrogen bond, but the other temperature coefficient values point to a limited degree of solvent shielding for the remaining NH groups. The $NH–CH^{\alpha}$ coupling constants are large (>8 Hz) for most residues and favour extended structures [23]. The solvent-shielded character of the internal NH protons could suggest the possibility that a certain amount of β-sheet conformation would contribute to the conformational equilibrium [23]. These findings agree with the FT-IR results discussed above.

Circular Dichroism

The far ultraviolet CD spectra of the oligomers $\mathbf{II}_{1-5}$ in TFE are shown in the left hand side of Figure 3. The spectra of all the glycopeptides, with the exception of $\mathbf{II}_1$, are characterized by a negative band at 190–195 nm and by a less intense positive band at 208–210 nm. An additional, extremely small, negative Cotton effect is visible near 230 nm.

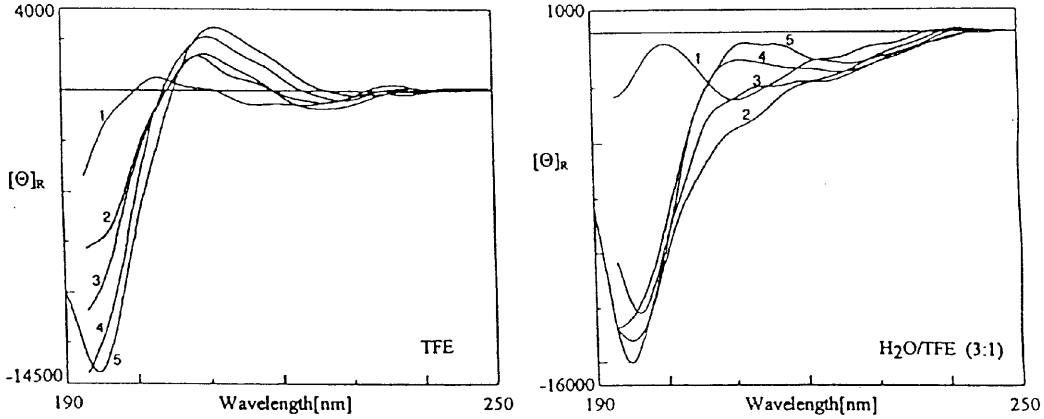

Figure 3 Far ultraviolet CD spectra of the Z-{[Gal(Ac)$_4\beta$]Thr}$_{1-5}$-NHCH$_3$ homo-peptides (**II**$_{1-5}$) at 298 K (concentration $\sim$ 1 mM in the indicated solvent).

By increasing the main-chain length, the bands increase their intensity and shift slightly to the red. In aqueous TFE solution (Figure 3, right) the **II**$_{2-5}$ oligomers exhibit a negative maximum at 195 nm and negative dichroic values in the n-π* region that, however, become less negative on going from **II**$_2$ to **II**$_5$. The CD spectra in TFE of the deacetylated oligomers of the series **III** (Figure 4, left), with the exception of **III**$_1$, show a negative band at 196–199 nm, a positive band at 214 nm and an isodichroic point at 204 nm. The intensity of both bands increases regularly with main-chain elongation. The spectra in aqueous solution (Figure 4, right) in the high-energy region (π–π*) are similar to those observed in TFE, whereas they show very weak negative dichroic values in the n–π* region. The steady variation of the dichroic bands of the homo-peptides of the series **II** and **III** underlines the absence of a conformational transition with increasing main-chain length. Under the same experimental conditions the conformation of the higher molecular weight glycopeptides of both series **II** and **III** becomes similar to those of poly-{[Gal(Ac)$_4\beta$]Thr} and poly-[(Galβ)Thr], respectively (Figure 5).

The CD spectra of **I**$_{1-4}$ in TFE (Figure 6, left) show that in the spectral region examined the ellipticity is always largely negative. The Cotton effect exhibited by **I**$_1$ is probably affected by contributions from the benzyl chromophore of the Z-blocking group [24]. The pattern of **I**$_2$ is characterized by a pronounced negative shoulder at approximately 215 nm, followed by a more intense maximum of the same sign near 195 nm. In the trimer and tetramer the intensity of the shoulder decreases. In aqueous TFE solution (Figure 6, right) the spectra of **I**$_3$ and **I**$_4$ exhibit minor variations, while **I**$_2$ shows an enhancement of both the n–π* and π–π* bands. A negative band near 200 nm is generally considered indicative of an essentially unordered conformation

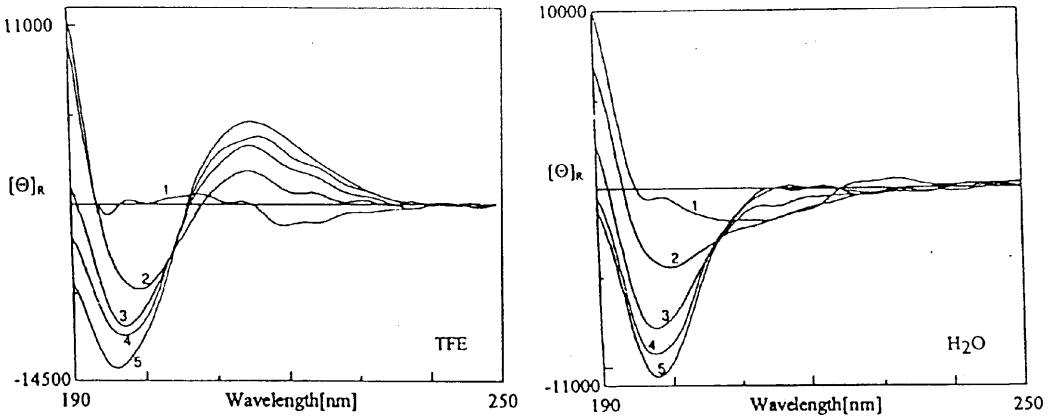

Figure 4 Far ultraviolet CD spectra of the Z-[(Galβ)Thr]$_{1-5}$-NHCH$_3$ homo-peptides (**III**$_{1-5}$) at 298 K (concentration $\sim$ 1 mM in the indicated solvent).

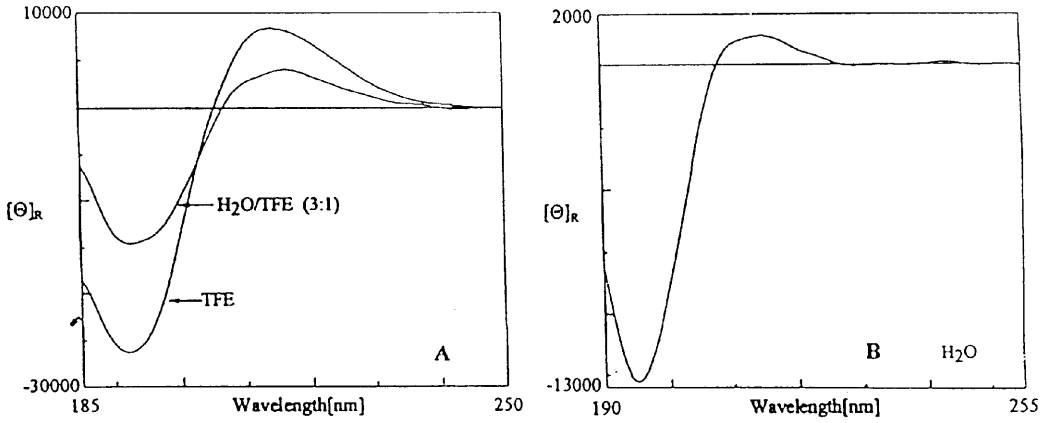

Figure 5 Far ultraviolet CD spectra of poly-{[Gal(Ac)$_4\beta$]Thr} (A) and poly-[(Galβ)Thr] (B) at 298 K in the indicated solvent.

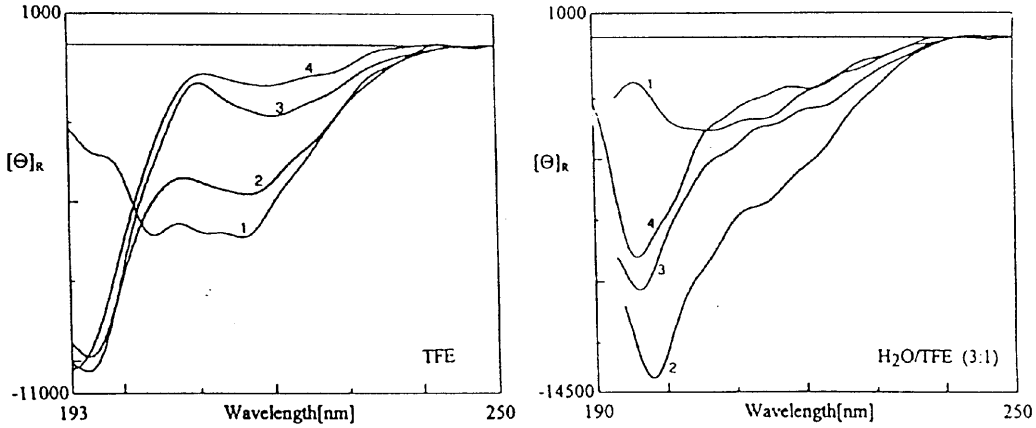

Figure 6 Far ultraviolet CD spectra of the Z-(Thr)$_{1-4}$-NHCH$_3$ homo-peptides (**I**$_{1-4}$) at 298 K (concentration $\sim$1mM in the indicated solvent).

[25]. The intensity of the π–π* band in the spectra of the series I$_{1-4}$, too small for a random coil conformation, could indicate the presence in the equilibrium mixture of a flexible, ordered structure. In conclusion, the CD spectra gave no additional information with respect to those obtained using ^{1}H-NMR and FT-IR.

CONCLUSIONS

The results of our investigations showed that, in the solvent of low polarity CDCl$_3$, the Thr homo-oligomers (series **I**) exhibit a marked tendency to aggregate, while a certain amount of aggregation is also possible in DMSO. There is no evidence for aggregation in CDC1$_3$ for the entire **II**$_{1-5}$ series in the concentration range 10–0.1 mM. In this solvent IR and NMR observations are consistent with the presence of intramolecularly hydrogen-bonded conformations in the **II**$_{1-5}$ oligomers, whereas, probably, C$_5$ and C$_7$ conformers coexist in the glycosylated and acetylated oligomers. In DMSO the amino and carboxy terminal NH groups are solvent exposed, while some relatively low dδ/dT values of the internal NH groups argue for an at least partial shielding of these groups from the solvent and, in the higher members of the **II** series, for an equilibrium between partially unordered structures and folded forms similar to those determined in CDCl$_3$.

In the series **III**, particularly in **III**$_5$, the internal NH groups are solvent-shielded in DMSO and strongly hydrogen-bonded. γ-Turns and hydrogen bondings different form ($i \leftarrow i+2$) interactions, involving the side-chain residues, may contribute to stabilizing a preferred conformation for the pentamer. Indeed, γ (C$_7$) conformations have been observed in relatively non-polar solvents [6, 15]. The onset of a γ-turn conformation, not frequently observed in DMSO [10], could be forced by the

sterically demanding requirements of the glycosylated and deacetylated Thr residues [26]. In this connection it is worth pointing out that sugars are frequently found in turn regions of proteins [27].

Acknowledgements

Financial support from the National Research Council (Progetto strategico 'Tecnologie Chimiche Innovative') and MURST of Italy is gratefully acknowledged. We thank Mr. F. Cavaggion for skillful technical assistance.

REFERENCES

1. L. Biondi, F. Filira, M. Gobbo, A. Polese, B. Scolaro and R. Rocchi in: *Peptides 1994*, H. L. S. Maia, Ed., p. 723–274, ESCOM, Leiden 1995.
2. C. Somlai, G. Szokan and L. Balaspiri (1992). Efficient, racemization-free amidation of protected amino acids. *Synthesis* 825–827.
3. E. Von Arx, M. Faupel and M. Brugger (1976). Das 4,4′-tetramethyldiamino diphenylmethan reagens (TDM). Eine modifikation der chlor-*o*-tolidin farbereaktion für die dünnschichtchromatographie. *J. Chromat. 120*, 224–228.
4. F. Filira, L. Biondi, F. Cavaggion, B. Scolaro and R. Rocchi (1990). Synthesis of *O*-glycosylated tuftsins by utilizing threonine derivatives containing an unprotected monosaccharide moiety. *Int. J. Peptide Protein Res. 36,* 86–96.
5. A. Aubry, J. Protas, G. Boussard, M. Marraud and J. Néel (1978). Experimental conformational studies of two peptides containing α-aminoisobutyric acid. Crystal structure of *N*-acetyl-α-amino isobutyric acid methylamide. *Biopolymers 17,* 1693–1712.
6. A. W. Burgess and H. A. Scheraga (1973). Stable conformation of dipeptides. *Biopolymers 12,* 2177–2183.
7. C. Toniolo, M. Pantano, F. Formaggio, M. Crisma, G. M. Bonora, A. Aubry, D. Bayeul, A. Dautant, W. H. J. Boesten, H. E. Schoemaker and J. Kamphuis (1994). Onset of the fully extended conformation in (αMe)Leu derivatives and short peptides. *Int. J. Biol. Macromol. 16,* 7–14.
8. Ch. Pulla Rao, P. Balaram and C. N. R. Rao (1983). Infrared spectroscopy study of C_7 intramolecular hydrogen bonds in peptides. *Biopolymers 22,* 2091–2104.
9. P. A. Raj and P. Balaram (1985). Conformational effects on peptide aggregation in organic solvents: spectroscopic studes of two chemotactic tripeptide analogs. *Biopolymers 24,* 1131–1146.
10. Ch. Pulla Rao, R. Nagaraj, C. N. R. Rao and P. Balaram (1980). Infrared studies on the conformation of synthetic alamethicin fragments and model peptides containing α-aminoisobutyric acid. *Biochemistry 19,* 425–431.
11. C. Toniolo, G. M. Bonora, V. Barone, A. Bavoso, E. Benedetti, B. Di Blasio, P. Grimaldi, F. Lelij, V. Pavone and C. Pedone (1985). Conformation of pleionomers of α-aminoisobutyric acid. *Macromolecules 18,* 895–902.
12. T. Miyazawa (1967) in: *Poly-α-Amino Acids*, G. D. Fasman, Ed., p. 69–103, Dekker, New York 1967.
13. H. Kessler (1982). Conformation and biological activity of cyclic peptides. *Angew. Chem. Int. Ed. Engl. 21,* 512–523.
14. S. Prasad, R. B. Rao and P. Balaram (1995). Contrasting solution conformations of peptides containing α-α-dialkylated residues with linear and cyclic side chain. *Biopolymers 35,* 11–20.
15. A. A. Ribeiro, M. Goodman and F. Naider (1979). The preferred conformations of protected homodi- to homoheptamethionine peptides. *Int. J. Peptide Protein Res. 14,* 414–436.
16. E. S. Pysh and C. Toniolo (1977). Conformational analysis of protected norvaline oligopeptides by high resolution proton magnetic resonance. *J. Am. Chem. Soc. 99,* 6211–6219.
17. D. V. Reddy, B. Jagannadh, A. S. Dutta and A. C. Kunwar (1995). NMR studies on the structure of some cyclic and linear antagonists of luteinizing hormone-releasing homrone (LHRH). *Int. J. Peptide Protein Res. 46,* 9–17.
18. C. Toniolo, G. M. Bonora, A. Bavoso, E. Benedetti, B. Di Blasio, V. Pavone, C. Pedone, V. Barone, F. Lelj, M. T. Leplawy, K. Kaczmarek and A. Redlinski (1988), Structural versatility of peptides from $C^{\alpha,\alpha}$-dialkylated glycines. **II**. An IR absorption and ^{1}H-NMR study of homo-oligopeptides from $C^{\alpha-\alpha}$-diethylglycine. *Biopolymers 27,* 373–379.
19. K. D. Kopple, M. Ohnishi and A. Go (1969), Conformations of cyclic peptides. **III**. Cyclopentaglycyltyrosyl and related compounds. *J. Am. Chem. Soc. 91,* 4264–4272.
20. K. D. Kopple, M. Ohnishi and A. Go (1969). Conformations of cyclic peptides. IV. Nuclear magnetic resonance studies of cyclopentaglycyl-L-leucyl and cyclodiglycyl-L-histidyldiglycyl-L-tyrosyl. *Biochemistry 8,* 4087–4095.
21. K. D. Kopple and T. J. Schamper (1972). Proton magnetic resonance line broadening produced by association with a nitroxide radical in studies of amide and peptide conformation. *J. Am. Chem. Soc. 94,* 3644–3646.
22. A. Bundi, C. Grathwohl, J. Hochmann, R. M. Keller, G. Wagner and K. Wuthrich (1975). Proton NMR of the protected tetrapeptides Tfa-Gly-Gly-L-X-L-Ala-OCH_3, where X stands for one of the 20 common amino acids. *J. Magn. Res. 18,* 191–198.
23. R. Kishore and P. Balaram (1984). Cyclic bis-cystine peptides. Models for antiparallel β-sheet conformations. *J. Chem. Soc. Chem. Commun.* 778–779.

24. R. W. Woody (1985) in: *The Peptides, Analysis, Synthesis and Biology, Vol. 7,* S. Undefriend and J. Meienhofer, Eds., p. 15–144, Academic Press, new York 1985.
25. N. Greenfield and G. D. Fasman (1969). Computed circular dichroism spectra for the evaluation of protein conformation. *Biochemistry 8,* 4108–4116.
26. A. Hamilton Andreotti and D. Kahne (1993). Effects of glycosylation on peptide backbone conformation. *J. Am. Chem. Soc. 115,* 3352–3353.
27. H. Paulsen (1990). Syntheses, conformations and X-ray structure analyses of the saccharide chains from the core regions of glycoproteins. *Angew. Chem. Int. Ed. Engl. 29,* 832–839.

